Articles

Crystal Structures of the Klenow Fragment of DNA Polymerase I Complexed with Deoxynucleoside Triphosphate and Pyrophosphate†,‡

Lorena S. Beese,§ Jonathan M. Friedman, and Thomas A. Steitz*

Departments of Molecular Biophysics and Biochemistry and Chemistry and Howard Hughes Medical Institute, Yale University, New Haven, Connecticut 06511

Received May 6, 1993; Revised Manuscript Received September 17, 1993®

ABSTRACT: Crystal structures of the Klenow fragment (KF) of DNA polymerase I from *Escherichia coli* complexed with deoxynucleoside triphosphate (dNTP) or with pyrophosphate (PP_i) determined to 3.9-Å resolution by X-ray crystallography show these molecules binding within the cleft of the polymerase domain and surrounded by residues previously implicated in dNTP binding. The dNTP binds adjacent to the O-helix [Ollis, D. L., Brick, P., Hamlin, R., Xuong, N. G., & Steitz, T. A. (1985a) *Nature 313,* 762–766] with its triphosphate moiety anchored by three positively charged residues, Arg 754, Arg 682, and Lys 758, plus His 734 and Gln 708. The dNTP binding site observed in the crystal is consistent with the results of chemical modification including cross-linking and is also near many of the amino acid residues whose mutation affects catalysis [Polesky, A. H., Steitz, T. A., Grindley, N. D. F., & Joyce, C. M. (1990) *J. Biol. Chem. 265,* 14579–14591; Polesky, A. H., Dahlberg, M. E., Benkovic, S. J., Grindley, N. D. F., & Joyce, C. M. (1992) *J. Biol. Chem. 267,* 8417–8428]. However, we conclude that the position of at least the dNMP moiety of dNTP in the binary complex is not likely to be the same as in its catalytically relevant complex with primer-template DNA.

Although DNA polymerase I from *Escherichia coli* (Pol I)[1] has been a paradigm for understanding the mechanism of DNA replication, little is established concerning the structures of substrates bound to the polymerase's active site. We describe, here, the structures of deoxynucleoside triphosphate bound to the polymerase. Pol I is a single polypeptide enzyme with three activities: a template-directed DNA polymerase, a 3′ to 5′ exonuclease which enhances the fidelity of DNA synthesis, and a 5′ to 3′ exonuclease. These three activities each reside on separate structural domains of the protein [reviewed in Joyce and Steitz (1987), Beese and Steitz (1989), and Kornberg and Baker (1992)]. Partial proteolysis cleaves the enzyme into two fragments; the amino-terminal proteolytic fragment contains the 5′ to 3′ exonuclease activity, while the larger, carboxy-terminal fragment [often referred to as the Klenow fragment (KF)] retains both DNA polymerase and 3′ to 5′ editing exonuclease capabilities (Brutlag *et al.*, 1969; Klenow & Henningsen, 1970).

The combination of results from X-ray crystallography (Ollis *et al.*, 1985a), site-directed mutagenesis (Freemont *et al.*, 1987; Derbyshire *et al.*, 1988, 1991; Polesky *et al.*, 1990, 1992), and biochemical and enzyme kinetic studies (Cowart *et al.*, 1989; Catalano *et al.*, 1990; Guest *et al.*, 1991) establishes that the DNA polymerase and 3′ to 5′ exonuclease active sites reside on different structural domains of the Klenow fragment, with about 30–35 Å separating them. The crystal structures of KF complexed either with deoxynucleoside monophosphate (dNMP) or with single-stranded DNA bound in the 3′, 5′ exonuclease active site (Ollis *et al.*, 1985a; Freemont *et al.*, 1988; Beese & Steitz, 1991) have led to a proposed enzymatic mechanism (Freemont *et al.*, 1988; Beese & Steitz, 1991) that is consistent with the results of extensive site-directed mutagenesis of the residues constituting the exonuclea se active site (Derbyshire *et al.*, 1988, 1991).

By contrast, the structural details of how the polymerase executes template-directed DNA synthesis have remained elusive. Crystal structures of KF complexed with substrates and products of the polymerase reaction have been difficult to obtain, due in part to the experimentally observed decrease in deoxynucleoside triphosphate (dNTP) and DNA binding affinity with increasing ionic strength (Englund *et al.*, 1969; Zimmerman & Harrison, 1987). KF crystallizes from very high ionic strength solutions (about 1.4 M sodium citrate) where dNTP and DNA binding is weak. Establishing the location of the binding sites for these substrates by diffusing them into these crystals at high salt concentrations have proved not possible. Formation of a crystalline complex has required transferring crystals into a low ionic strength buffer before diffusing in substrates, or growing crystals under low ionic strength conditions in the presence of substrates. Biochemical and molecular genetic studies have characterized the binding of dNTP to the polymerase's active site. Equilibrium (Englund *et al.*, 1969) and nonequilibrium dialysis studies (Muise & Holler, 1985) demonstrated that dNTPs bind to a single site with dissociation constants which range between 10^{-5} and 10^{-4} M. Chemical modification and cross-linking (Pandey *et al.*, 1987; Pandey & Modal, 1988; Rush *et al.*, 1990; Basu &

† This work was supported by American Cancer Society Grant NP-421 to T.A.S.

‡ Crystallographic coordinates of the Klenow fragment complexed with dCTP have been deposited in the Brookhaven Protein Data Bank under the filename 1KFD.

* To whom correspondence should be addressed at the Department of Molecular Biophysics and Biochemistry.

§ Current address: Department of Biochemistry, Duke University Medical Center, Durham, NC 27710.

® Abstract published in *Advance ACS Abstracts,* November 15, 1993.

[1] Abbreviations: Pol I, DNA polymerase I from *Escherichia coli*; KF, the Klenow fragment of *E. coli* DNA polymerase I; dNTP, deoxynucleosoide 5′-triphosphate; PP_i, inorganic pyrophosphate; dCTP, deoxycytosine 5′-triphosphate; dTTP, thymidine 5′-triphosphate; ATP, adenosine triphosphate; dNMP, deoxynucleoside 5′-monophosphate.

0006-2960/93/0432-14095$04.00/0

Modak, 1987) as well as site-directed mutagenesis studies (Polesky *et al.*, 1990, 1992) have placed certain amino acid residues in proximity to the dNTP binding site, localizing it in the large cleft of KF.

We report here the crystal structures of several binary complexes of KF with dNTPs and with pyrophosphate. Whilethese binary complex structures are entirely consistent with data from solution experiments, the relationship of these complexes to the structure of dNTP bound in a ternary complex that includes DNA is less clear.

EXPERIMENTAL PROCEDURES

Crystallization and Data Collection. Klenow fragment protein was overexpressed in *E. coli* using the λ-P_L phage system developed by Joyce and Grindley (1983) and purified as described by Derbyshire *et al.* (1991). Crystals were grown by combined equilibrium dialysis and vapor diffusion from 1.4 M sodium citrate buffer, pH 5.8, as described in Brick *et al.* (1983). Harvested crystals were transferred into a stabilizing buffer containing 70% saturated ammonium sulfate and 66 mM PIPES buffer, pH 7.0, with 20 mM $MgSO_4$. Crystals belong to the tetragonal space group $P4_3$ and have one molecule of MW 68 000 per asymmetric unit. The unit cell dimensions are $a = b = 103.8$ Å and $c = 86.0$ Å.

Initially, nucleoside triphosphate and pyrophosphate (PP_i) were bound by soaking these crystals in very high concentrations of ATP and PP_i. Crystals were transferred in several steps into buffers containing either 0.75 M ATP and 50 mM $MnCl_2$, pH 6.4, or 0.9 M $NaPP_i$ and 20 mM $MnCl_2$, pH 6.4. X-ray diffraction data were collected to 7-Å resolution on a modified Picker diffractometer.

Subsequently, crystals of KF were transferred into a low ionic strength precipitant following the approach described by Schreuder *et al.* (1988). Hanging drop equilibration was used to estimate the concentration of low ionic strength precipitant that could substitute for the high ionic strength crystal stabilization buffer. The rationale behind this approach is to adjust the activity of water in any alternative crystal stabilization solution to approximate the water activity of the original solution. Crystals of KF were stabilized by 44% poly(ethylene glycol) MW 6000 (44 g of PEG 6000 in 56 g of buffer solution), 50 mM PIPES, pH 7.0, and 10 mM $MgSO_4$. The transfers were complicated by the fact that solutions of 70% saturated ammonium sulfate and 44% PEG 6000 are immiscible. Any visible ammonium sulfate solution adhering to the surface of the transferred crystal was removed, and removal was repeated during equilibration of the crystal with the new stabilization solution as discussed in Schreuder *et al.* (1988). Although crystals initially cracked, they subsequently reannealed. Not all crystals in a batch could be transferred successfully by this technique. Many crystals cracked, failed to anneal, and eventually lost all birefringence. The degree of success appeared to depend on how quickly the pool of ammonium sulfate solution could be removed from around the transferred crystal. Crystal that survived the initial transfer and equilibration were subsequently transferred into 44% PEG 6000 and 50 mM PIPES, pH 7, containing either 1 mM dCTP and 10 mM $MgSO_4$, 1 mM dTTP and 5 mM $MnSO_4$, 1 mM dTTP and 5 mM $MgSO_4$, 5 mM dTTP, 5 mM dTMP, and 5 mM $MnSO_4$, or 10 mM sodium pyrophosphate and 10 mM $MgSO_4$. X-ray diffraction data were collected using a Mark II two-dimensional position-sensitive area detector (Xuong *et al.*, 1985) at 10 °C.

Crystals of KF have also been grown under low ionic strength conditions from solutions containing 7% PEG 6000 in the presence of DNA and the dTTP analogue, thymidine, α,β-methylenetriphosphate or 5-iodouridine α,β-methylenetriphosphate. Under these conditions the ionic strength is determined by the concentration of buffer, which varied from 0.02 to 0.1 M in the studies described herein. These crystals are of space group $P3_221$ with unit cell dimensions $a = b = 112$ Å and $c = 138.3$ Å. Further descriptions of the growth and structure determination of these crystals shall appear elsewhere (Friedman, Beese, and Steitz, in preparation). X-ray diffraction data were collected using a Mark II two-dimensional position-sensitive area detector (Xuong *et al.*, 1985) at −20 °C.

Crystallographic Data Analysis. In general, the diffraction pattern of the crystals grown at high ionic strength became weaker upon their transfer into PEG buffer. Typically, the average signal to noise of the diffraction intensities, $\langle I \rangle / \langle \sigma I \rangle$, dropped below 2 at 3.5-Å resolution for transferred crystals rather than the 2.5 Å observed at high ionic strength crystals. Transfer into low ionic strength often resulted in unit cell dimension changes that varied significantly from crystal to crystal.

One crystal of a dCTP–KF complex had the same unit cell dimensions as apo-KF crystals in 70% saturated ammonium sulfate, which allowed its diffraction intensities to be scaled to intensities from an apo-KF crystal. At 3.9-Å resolution, the fractional isomorphous difference $(\sum_h |I_{hD} - I_{hN}| / \sum_h |I_{hD} + I_{hN}|$, where I_D and I_N are the observed diffraction intensities of the complexed protein and apoprotein, respectively) between these two data sets is 0.12. A difference electron density map calculated using the diffraction amplitudes of the dCTP–KF complex minus those of the uncomplexed protein and phases calculated from the refined KF model (Figure 1) allowed fitting of dCTP using the interactive graphics program FRODO (Jones, 1985).

Crystals of KF complexed with Mg–dTTP, Mn–dTTP and dTMP, Mn–dTTP, Mg–PP_i, and other crystals with dCTP were not isomorphous with each other or with crystals of apo-KF in 70% saturated ammonium sulfate. The transfer into low ionic strength buffer appears to slightly disrupt the crystal packing. For example, comparison of diffraction intensities measured from the Mn–dTTP complex with those from crystals in 70% saturated ammonium sulfate shows 38% isomorphous differences to 3.4-Å resolution. The *a* and *b* unit cell lengths increased by about 1%. Rigid body refinement of the protein structure from the "high-salt" lattice into the "low-salt" lattice was required to calculate an interpretable difference electron density map. Rigid body refinement using X-PLOR (Brünger, 1990) reduced the *R* factor $[R = \sum(|F_c| - |F_o|) / \sum |F_o|]$ between observed and calculated structure factors from 0.38 to 0.24 for 8704 unique reflections between 20- and 3.4-Å resolution. This corresponds to about 85% of the diffraction data to 3.4 Å. The molecule was rotated by 1° with respect to apo-KF in the high-salt lattice. Difference electron density maps were calculated using as coefficients $F_{complex} - F_{apo,calcd}$ and calculated phases (Table I).

The crystal form in space group $P3_221$ grown at low salt had an anisotropic diffraction pattern extending to about 3.8-Å resolution in the a^* direction and 4.5 Å in the perpendicular direction. Diffraction intensities measured from crystals complexed with the iodinated dUTP analogue and those grown in the presence of the dTTP analogue merged with *R* factors of 8% and 10%, respectively. The structure of the trigonal form was solved by molecular replacement using the coordinates derived from the tetragonal crystal form (J. M. Friedman, L. S. Beese, and T. A. Steitz, in preparation).

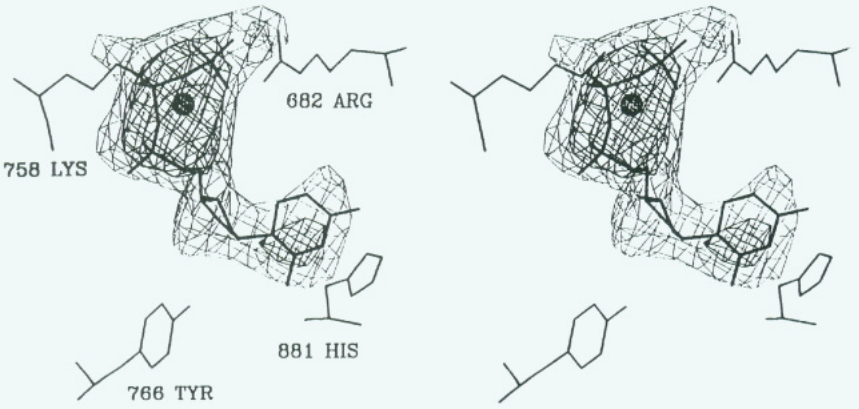

FIGURE 1: Difference electron density map calculated at 3.9-Å resolution using diffraction amplitudes of the dCTP–KF complex minus those of the uncomplexed protein and phases derived from the refined KF structure. dCTP is fit into the positive electron density which is contoured at 3σ and 4σ, where σ is the root-mean-square density throughout the unit cell. Mg^{2+} is represented by a dotted sphere. Residues Lys 758, Arg 682, Tyr 766, and His 881 form part of the dNTP binding site, which is consistent with previous solution studies.

Table I: Crystallographic Data Analysis

crystals	resolution, Å	no. of unique reflections	R_{merge},[a] %	R factor[b]
KF–dTTP	3.4	8700	7.7	0.24[c]
KF–dCTP	3.9	5800	6.4	
KF–dTTP and –dTMP	3.5	8300	6.1	0.23[c]
KF–PP_i	4.0	4900	8.9	0.25[c]
KF–dTMP	2.5	21100	5.1	0.198[d]

[a] $R_{merge} = \sum_h(\sum_i|I_{ih} - \langle I_h\rangle|)/\sum_h\langle I_{ih}\rangle$, where I_h = intensity of the ith observation of reflection h. [b] R factor = $\sum(|F_c|-|F_o|)/\sum|F_o|$, where F_c and F_o are calculated and observed structure factors, respectively. [c] Calculated after rigid body refinement using X-PLOR (Brünger, 1991) where the refined KF–dTMP structure was rotated into the observed lattice of the complex. [d] Calculated after full positional refinement using PROLSQ and X-PLOR (Beese & Steitz, 1991; Beese and Steitz, in preparation). rms deviation of bond lengths and bond angles from ideality is 0.015 Å and 2.9°, respectively.

RESULTS

dNTP Binding Site. The dNTP binding site lies within the cleft of the polymerase domain (Figure 2) near residues whose mutation affects catalysis (Polesky *et al.*, 1990, 1992). Although the precise position of each phosphate group and the magnesium ion cannot be determined unambiguously at 3.9-Å resolution, the triphosphate portion of the Mg–dCTP was fit into the highest electron density of a difference Fourier between the complex and the apoenzyme (Figure 1). Consequently, constraints derived from other studies were also used to construct a model of the bound substrate. The Mg^{2+} was built as a bidentate chelate β,γ-phosphate since this interaction has been suggested for the active dNTP substrate (Sloan *et al.*, 1975; Burgers & Eckstein, 1979; Mullen *et al.*, 1989). The phosphate oxygens were positioned within 3.8 Å of the positively charged side chain of Lys 758 and near that of Arg 754 on the O-helix of the polymerase domain (Figure 3). The side chains of residues His 734, Gln 708, and Arg 682 are also close enough to interact with a phosphate group.

It is sometimes possible to obtain detailed information about the position of Mg^{2+} by replacing it with Mn^{2+}, relying both on the difference in the electron densities of these metal ions and on anomalous scattering. The difference electron density map of a Mn–dTTP complex calculated at 3.4-Å resolution is almost identical to that of the Mg–dCTP complex in the region where triphosphate was positioned in the electron density (Figure 4). Unfortunately, it proved not possible to determine the position of Mg^{2+} directly by replacing it with Mn^{2+}. Since the Mg–dCTP and Mn–dTTP crystals are not isomorphous, it was not possible to calculate a difference map using measured diffraction amplitudes. Further, measurements of the anomalous scattering differences from the Mn–dTTP complex were of insufficient quality to produce an interpretable anomalous difference Fourier.

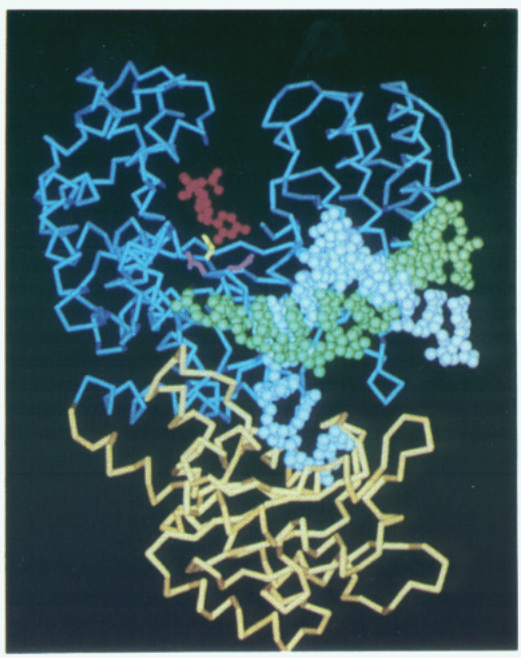

FIGURE 2: α-Carbon backbone representation of KF with DNA bound in an editing complex (Beese *et al.*, 1993) with dCTP bound to the polymerase active site. The dCTP is shown in red, the primer strand is shown in white, and the template strand is shown in green. The polymerase and 3′, 5′ exonuclease domains are shown in blue and yellow, respectively. Residues Asp 882 and Glu 883 are shown in pink, and Asp 705 is in yellow. These residues are highly conserved among all polymerases, and mutations in any of these residues significantly affect catalysis.

Comparisons of difference electron density maps of dNTP complexes obtained from different soaking experiments indicate that the precise orientation of the base depends on the conditions of the experiment. In the Mg–dCTP complex, cytosine interacts with His 881, while the sugar interacts with Phe 764 (Figures 3 and 5). In the binary complexes with Mn–dTTP or Mg–dTTP the base appears to point toward Tyr 766 (Figures 4 and 5) although the position for thymidine is much less well determined. In general, the difference maps can best be explained by assuming that the base is bound less specifically than the phosphates and is able to adopt multiple

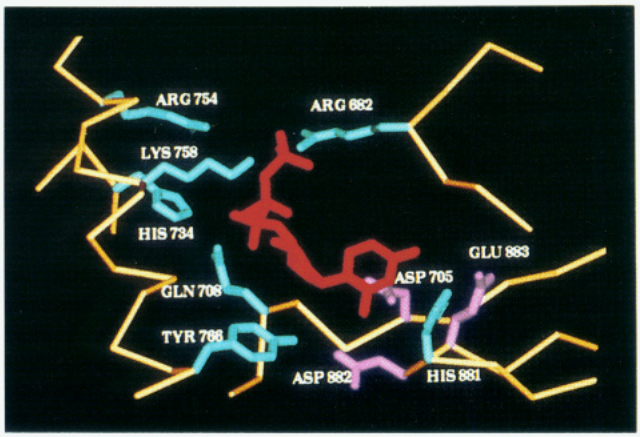

FIGURE 3: dCTP binding site. Residues that interact with dCTP are shown in blue. Residues Asp 882, Glu 883, and Asp 705 that are highly conserved among all polymerases and whose mutations significantly affect catalysis are shown in purple.

conformations.

Data from crystals in the space group $P3_221$ grown from low ionic strength buffer in the presence of a DNA and dNTP analogue suggest a similar position of dNTP binding. A difference map between the iodinated and uniodinated α,β-methylene analogues of dUTP complexed with KF shows an iodine atom in the cleft near His 881, a position consistent with that of the base seen in the dCTP complex (Figure 5). Electron density for the triphosphate group is observed in an electron density map calculated using $2F_o - F_c$ as coefficients and phases calculated from the model positioned by molecular replacement. Duplex DNA, although present in the crystallization, is not visible in the electron density maps, suggesting that it is disordered in these crystals.

The position of the deoxynucleoside triphosphate observed at low ionic strength is consistent with experiments in which crystals of KF grown from high ionic strength buffer were transferred into 0.75 M Mn–ATP. A difference electron density map calculated at 7-Å resolution shows the same binding site for ATP as observed for dTTP at low ionic strength. The position of the triphosphate group observed at high ionic strength overlaps with that observed at low ionic strength. A difference electron density map between Mn–ATP and Mn–PP_i complexes suggests that adenosine monophosphate points toward Tyr 766 in a manner similar to that observed in the low ionic strength Mg–dTTP and Mn–dTTP complexes (Figures 4 and 5).

PP_i Binding Site. The difference electron density map between the Mg–PP_i–KF complex and apo-KF calculated at 4-Å resolution implies that the pyrophosphate anion binds in the cleft of the polymerase domain and appears to interact with a cluster of positively charged amino acids, Lys 758, Arg 754, and His 734 (Figure 6). The density into which the Mg–PP_i is fit partially overlaps with the electron density attributed to the β- and γ-phosphate groups in the dNTP complexes. At 4-Å resolution the phosphate groups and the magnesium cation cannot be distinguished or accurately positioned. The model was therefore fit into the electron density so as to maximize the number of hydrogen bonds formed between the PP_i group and the amino acid side chains.

The pyrophosphate binding site observed in the tetragonal crystals that were transferred to low ionic strength is the same as the site observed when these crystals are transferred to solutions containing 0.9 M sodium pyrophosphate. Only one binding site for PP_i is observed even at these extremely high concentrations of PP_i.

dNTP Binding Site at the 3′ to 5′ Exonuclease Active Site. At 5 mM concentrations of dTTP and dTMP, a second binding site for dTTP is found near the 3′ to 5′ exonuclease active site (Figure 7). This secondary dNTP binding site overlaps with the site for single-stranded DNA and is approximately the same binding site as the third nucleotide from the 3′ end of a single strand of DNA (Beese & Steitz, 1991).

DISCUSSION

Comparison of dNTP Binding Site with Biochemical Studies. The dNTP binding site observed in the crystalline Klenow fragment is consistent with earlier solution studies of the binary complex between *E. coli* DNA polymerase I and dNTP, suggesting that the mode of dNTP binding observed in the crystal is identical with that formed in solution. The inhibition of DNA polymerase activity that results from the cross-linking of 5′-(fluorosulfonylbenzoyl)deoxyadenosine to Arg 682 was interpreted by Pandey and Modak (1988) to mean that Arg 682 interacts with the β- or γ-phosphate group of dNTP. Similarly, the inhibition of polymerase activity, but not DNA binding, upon the covalent modification of Lys 758 with pyridoxal phosphate suggests that Lys 758 also binds a phosphate group of dNTP (Basu & Modak, 1987). Both Lys 758 and Arg 682 interact with phosphate groups of dNTP in the crystal.

Several experiments have identified residues that interact with the base in a binary complex with dNTP. Photoaffinity cross-linking of 8-azido-dATP to KF selectively modifies Tyr 766 (Rush & Konigsberg, 1990). Pandey *et al.* (1987) identify His 881 as the site for a specific UV-mediated cross-linking to a dTTP derivative. Since His 881 and Tyr 766 are separated by more than 9 Å, it is unlikely that a single orientation of the base moiety could account for the selective chemical modification of both amino acid residues. Instead, the crystallographic data suggest that, in the absence of DNA primer and template, the base and sugar moieties of dNTP's are able to adopt multiple conformations.

Previous studies of DNA polymerase I suggested that the triphosphate moiety of dNTP is of primary importance for binding specificity in formation of the binary complex with KF. The sugar and base groups contribute far less to substrate specificity since bulky base analogues are accommodated at the dNTP binding site [reviewed in Kornberg and Baker (1992)]. In addition, the significance of ionic interactions between the triphosphate group and the protein is consistent with the observed increase of K_m(dNTP) with increasing ionic strength (Englund *et al.*, 1969; Zimmerman & Harrison, 1987).

Mullen *et al.* (1989) have reported binding of dNTP to an oligopeptide which includes amino acid residues in the *O*-helix that we observe binding the triphosphate. It should be pointed out, however, that the three-dimensional structure assumed by this short peptide in solution and established by NMR is different from the structure of this peptide present in the whole molecule as established in the crystal structure.

The recently proposed model of dNTP substrate and primer-template DNA bound to KF by Yadav *et al.*, (1992) is not correct and should be disregarded. First, and most important, the protein side chains were incorrectly model built from the α-carbon backbone, making all subsequent conclusions in error. Second, the position and orientation of the dNTP are not as observed in the crystalline binary complex or as we anticipate for the ternary complex: the phosphates and the sugar–base are interchanged in position. Third, the direction of approach of the primer strand to the active site cleft is inconsistent with the observed position of duplex DNA in a KF–DNA cocrystal

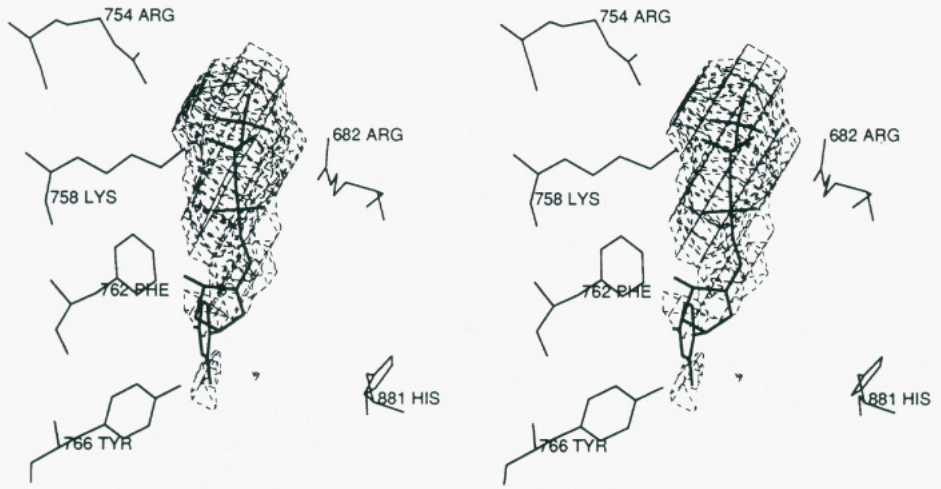

FIGURE 4: A portion of the difference electron density map calculated to 3.4-Å resolution between dTTP–KF and uncomplexed KF. The dTTP complex was formed in the presence of 5 mM $MnSO_4$. The map was calculated using the observed dTTP–KF amplitudes (F_o) minus those calculated from the refined uncomplexed KF structure after rigid body refinement into the dTTP–KF lattice (F_c) using phases derived from the refined KF structure. dTTP is fit into the positive electron density which is contoured at 2σ and 4σ.

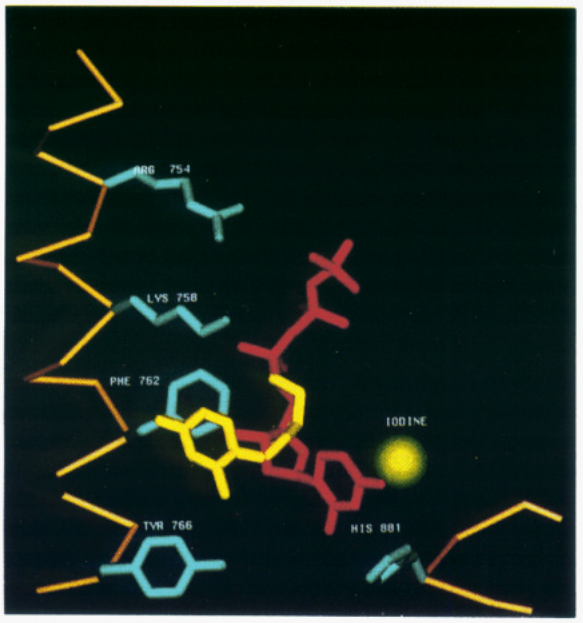

FIGURE 5: Two orientations of the sugar and base moieties of dNTP. The orientation of the sugar and base of complexed dTTP is shown in yellow and dCTP is shown in red. The triphosphate moiety of dTTP is in approximately the same position observed in the dCTP complex. Residues along the O-helix and His 881 that interact with dNTP are shown in blue. The position of an iodine atom determined from a difference map between the iodinated and uniodinated α,β-methylene analogues of dUTP is indicated by a green sphere.

structure (Figure 2; Beese *et al.*, 1993). Finally, the steric overlaps between substrates and the protein model are significant.

dNTP Binding at the Exonuclease Site. A second, lower affinity binding site for dNTP lies at the 3′ to 5′ exonuclease active site and positions the base of dTTP within 5 Å of that of dTMP. The binding of dTMP and the position of side chains at the active site are unchanged from what has been previously reported (Ollis *et al.*, 1985a; Beese *et al.*, 1991). The secondary dNTP binding site, observed only at higher concentrations of dNTP and in the presence of dNMP, explains the ^{1}H NMR paramagnetic relaxation study of Krugh (1971), who concluded that the binding sites for dNTP and dNMP were within 5 Å of one another. Although no effect was observed until the concentration of the spin-labeled dNTP was about 1 mM, it was argued that this higher K_D arose from structural differences between the spin-labeled substrate and unmodified dNTP's. The result of this NMR paramagnetic relaxation study led to the interpretation that the 3′ to 5′ exonuclease active site (marked by the dNMP) and polymerase active site (marked by the spin-labeled dNTP) were adjacent on the surface of the enzyme. Our present crystallographic results suggest that the NMR experiment was detecting a secondary binding site which is occupied only at higher concentrations of dNTP. A spin-labeled dNTP bound at the polymerase active site would have been about 35 Å away from the dNMP, too far to affect the line widths of the C2′ and C3′ 1-H resonances of dNMP.

Primary Sequence Similarities and Site-Directed Mutagenesis. Amino acid residues near the observed dNTP binding site in the KF are conserved among both prokaryotic (Ollis *et al.*, 1985b; Argos *et al.*, 1986; Braithwaite & Ito, 1993) and eukaryotic (Delarue *et al.*, 1990; Wang *et al.*, 1989; Braithwaite & Ito, 1993) DNA polymerases. The dNTP lies close to residues emanating from three motifs (A, B, and C) whose sequence is conserved among the DNA-dependent polymerases (Delarue *et al.*, 1990). The α-phosphate of the dNTP is 6 Å from Asp 882 (an invariant residue in motif C) and Asp 705 (an invariant residue in motif A), midway between the two positions (Figures 2 and 3). Both of these residues have been shown by site-directed mutagenesis to be essential for catalysis (Polesky *et al.*, 1990, 1992). The dNTP binds along the O-helix which includes residues from motif B. However, although close to these conserved and catalytic residues, the dNTP binding site is not actually in direct contact with these residues.

Most of the residues in the dNTP binding cleft that are conserved among prokaryotic polymerases and are solvent exposed have been changed using site-directed mutagenesis and the consequences accessed (Polesky *et al.*, 1990, 1992). Mutation of Asn 845, Arg 841, or Tyr 766 causes an increase in K_m(dNTP), which may imply that these residues interact with some part of the incoming dNTP molecule (Polesky *et al.*, 1990). However, the 2–5-fold increase in K_m(dNTP) is rather small and could also be explained by a perturbation of DNA template binding. Although Tyr 766 interacts with dNTP in the binary complex, residues Asn 845 and Arg 841 are too far away to contact the dNTP. Since the distance between Asn 845 and Arg 841 and residues Lys 758 or Arg

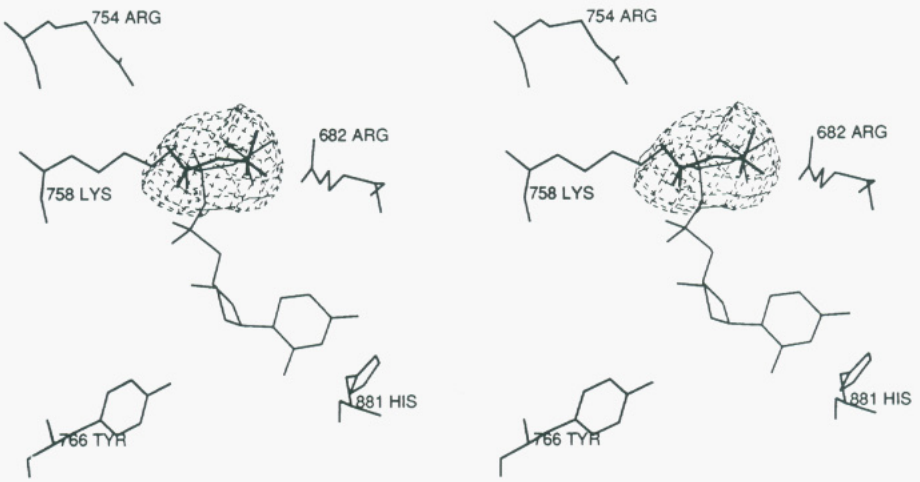

FIGURE 6: Difference electron density map between PP_i–KF and uncomplexed KF calculated to 4.0-Å resolution. The map was calculated using the observed PP_i–KF amplitudes (F_o) minus those calculated from the refined uncomplexed KF structure after rigid body refinement into the PP_i–KF lattice (F_c) using phases derived from the refined KF structure. PP_i is fit into the positive electron density which is contoured at 4σ. The position of the dCTP ligand is included for comparison.

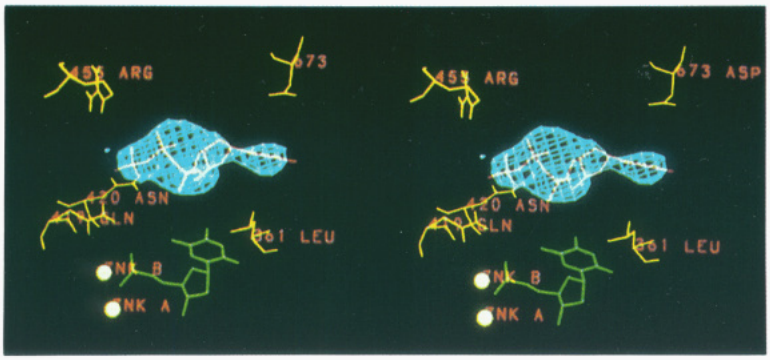

FIGURE 7: Lower affinity second binding site for dNTP located near the 3′, 5′ exonuclease active site adjacent to the binding site for dNMP. A portion of the 3.5-Å resolution difference electron density map between a complex of KF containing both dTTP and dTMP and KF complexed with only dTMP is shown. The map was calculated using the observed dTTP, dTMP–KF amplitudes (F_o) minus those calculated from the refined dTMP–KF structure after rigid body refinement into the dTTP, dTMP–KF lattice (F_o) using phases derived from the refined dTMP–KF structure. dTTP (shown in red) is fit into the positive electron density contoured at 2σ. dTMP is shown in green. The two spheres (Znk A and Znk B) mark the positions of the two divalent metal ions that are essential for exonuclease activity.

668 is larger than could be spanned by a single dNTP in a reasonable conformation, all of these residues cannot form part of the dNTP binding site.

Relationship between dNTP Binding Site in Binary and Ternary Complexes. While the crystal structure of the binary complex clearly represents the complex that has been studied in solution, its relevance to the dNTP complex in the presence of primer and template DNA is less obvious. Since the entire binding site for the base of dNTP is formed by its Watson–Crick hydrogen bonding to the template strand and its stacking on the 3′ base of the primer strand, it is not unlikely that the binding site for the base in the binary complex is completely adventitious, consistent with our observation that it can bind in several locations dependent on conditions. Kinetic experiments indicate that dNTP forms a nonproductive complex with Pol I in the absence of DNA (Kuchta *et al.*, 1987). These kinetic experiments, however, cannot establish the extent to which the binding of dNTP differs in the binary and ternary complexes. Under single turnover polymerization conditions PP_i has been shown to be a competitive inhibitor of dNTP, suggesting that PP_i and dNTP bind to a similar location (Dahlberg & Benkovic, 1991). It is possible that the position of some or all of the phosphates of the triphosphate is the same in both binary and ternary complexes.

CONCLUSIONS

The binding site for dNTP observed in crystals of the binary complex is the same as observed in solution studies. However, extrapolating from this binary complex to a model for the complex with dNTP in the presence of primer and template DNA requires considerable caution. We presume that the sugar and base moiety of the dNTP require primer-template DNA to bind in correct conformation. On the basis of its proximity to conserved and catalytically important residues and the location of the PP_i binding site, we hypothesize that the observed position of the triphosphate moiety may be closely related to its position in the productive ternary complex.

ACKNOWLEDGMENT

We thank Drs. Catherine Joyce, Nigel Grindley, and Victoria Derbyshire for helpful discussions and Dr. N. Hamaguchi for assistance with Figures 2 and 3.

REFERENCES

Argos, P., Tucker, A. D., & Philipson, L. (1986) *Virology 149*, 208–216.

Atkinson, D. S., Deutscher, M. P., Kornberg, A., Russell, A. F., & Mofatt, J. G. (1969) *Biochemistry 8*, 4897–4904.

Basu, A., & Modak, M. J. (1987) *Biochemistry 26*, 1704–1709.

Basu, S., Basu, A., & Modak, M. J. (1988) *Biochemistry 27*, 6710–6716.
Beese, L. S., & Steitz, T. A. (1989) *Nucleic Acids and Molecular Biology* (Eckstein, F., & Lilley, D. M. J., Eds.) Vol. 3, pp 28–43, Springer-Verlag, Berlin.
Beese, L. S., & Steitz, T. A. (1991) *EMBO J. 10*, 25–33.
Beese, L. S., Derbyshire, V., & Steitz, T. A. (1993) *Science 260*, 353–355.
Braithwaite, D. K., & Ito, J. (1993) *Nucleic Acids Res. 21*, 787–802.
Brick, P., Ollis, D., & Steitz, T. A. (1983) *J. Mol. Biol. 166*, 453–456.
Brünger, A. (1990) *X-PLOR Manual, Version 2.1*, Yale University, New Haven, CT.
Brünger, A. T., Kuriyan, J., & Karplus, M. (1987) *Science 235*, 458–460.
Brutlag, D., Atkinson, M. R., Setlow, P., & Kornberg, A. (1969) *Biochem. Biophys. Res. Commun. 37*, 982–989.
Burgers, P. M. J., & Eckstein, F. (1979) *J. Biol. Chem. 254*, 6889–6893.
Catalano, C. E., Allen, D. J., & Benkovic, S. J. (1990) *Biochemistry 29*, 3612–3621.
Cowart, M., Gibson, K. S. Allen, D. J., & Benkovic, S. J. (1989) *Biochemistry 28*, 1975–1983.
Dahlberg, M. E., & Benkovic, S. J. (1991) *Biochemistry 30*, 4835–4843.
Delarue, M., Poch, O., Tordo, N., Moras, D., & Argos, P. (1990) *Protein Eng. 3*, 461–467.
Derbyshire, V., Freemont, P. S., Sanderson, M. R., Beese, L. S., Friedman, J. M., Steitz, T. A., & Joyce, C. M. (1988) *Science 240*, 199–201.
Derbyshire, V., Grindley, N. D. F., & Joyce, C. M. (1991) *EMBO J. 10*, 17–24.
Englund, P. T., Huberman, J. A., Jovin, T. M., & Kornberg, A. (1969) *J. Biol. Chem. 244*, 3038–3044.
Freemont, P. S., Ollis, D. L., Steitz, T. A., & Joyce, C. M. (1986) *Proteins 1*, 66–73.
Freemont, P. S., Friedman, J. M., Beese, L. S., Sanderson, M. R., & Steitz, T. A. (1988) *Proc. Natl. Acad. Sci. U.S.A. 85*, 8924–8928.
Guest, C. R., Hochstrasser, R. A., Dupuy, C. G., Allen, D. J., Benkovic, S. J., & Millar, D. P. (1991) *Biochemistry 30*, 8759–8770.
Jones, T. A. (1985) *Methods Enzymol. 115*, 157–171.
Joyce, C. M., & Grindley, N. D. F. (1983) *Proc. Natl. Acad. Sci. U.S.A. 80*, 1830–1834.
Joyce, C. M., & Steitz, T. A. (1987) *Trends Biochem. Sci. 12*, 288–292.
Klenow, H., & Henningsen, I. (1970) *Proc. Natl. Acad. Sci. U.S.A. 65*, 168–175.
Kornberg, A., & Baker, T. (1992) *DNA Replication*, 2nd ed., A. H. Freeman and Co., New York.
Krugh, T. A. (1971) *Biochemistry 10*, 2594–2599.
Kuchta, R. D., Mizrahi, V., Benkovic, P. A., Johnson, K. A., & Benkovic, S. J. (1987) *Biochemistry 26*, 8410–8417.
Mohan, P. M., Basu, A., Basu, S., Abraham, K. I., & Modak, M. J. (1988) *Biochemistry 27*, 226–233.
Muise, O., & Holler, E. (1985) *Biochemistry 24*, 3618–3622.
Mullen, G. P., Shenbagamurthi, P., & Mildvan, A. S. (1989) *J. Biol. Chem. 264*, 19637–19647.
Ollis, D. L., Brick, P., Hamlin, R., Xuong, N. G., & Steitz, T. A. (1985a) *Nature 313*, 762–766.
Ollis, D. L., Kline, C., & Steitz, T. A. (1985b) *Nature 313*, 818–819.
Pandey, V. N., & Modal, M. J. (1988) *J. Biol. Chem. 263*, 6068–6073.
Pandey, V. N., Williams, K. R., Stone, K. L., & Modak, M. J. (1987) *Biochemistry 26*, 7744–7748.
Polesky, A. H., Steitz, T. A., Grindley, N. D. F., & Joyce, C. M. (1990) *J. Biol. Chem. 265*, 14579–14591.
Polesky, A. H., Dahlberg, M. E., Benkovic, S. J., Grindley, N. D. F., & Joyce, C. M. (1992) *J. Biol. Chem. 267*, 8417–8428.
Rush, J., & Konigsberg, W. H. (1990) *J. Biol. Chem. 265*, 4821–4827.
Schreuder, H. A., Groendijk, H., van der Laan, J. M., & Wierenga, R. K. (1988) *J. Appl. Crystallogr. 21*, 426–429.
Sloan, D. L., Loeb, L. A., Mildvan, A. S., & Feldman, R. J. (1975) *J. Biol. Chem. 250*, 8913–8920.
Wang, T. S. F., Wong, S. W., & Korn, D. (1989) *FASEB J. 3*, 14–21.
Xuong, N. H., Nielson, C., Hamlin, R., & Anderson, D. (1985) *J. Appl. Crystallogr. 18*, 342–350.
Yadav, P. N. S., Yadav, J. S., & Modak, M. J. (1992) *Biochemistry 31*, 2879–2886.
Zimmerman, S. B., & Harrison, B. (1987) *Proc. Natl. Acad. Sci. U.S.A. 84*, 1871–1875.